

# Molecular Dynamics Study of Ionic Melts Resulting from Contact Melting

E. A. Goncharenko\*, T. A. Grechukha\*, P. F. Zil'berman\*\*, and V. S. Znamenskii\*\*

\* Kabardino-Balkar State University, ul. Chernyshevskogo 173, Nalchik, 360004 Russia

\*\* Kabardino-Balkar State Agricultural Academy, ul. Tolstogo 185, Nalchik, 360004 Russia

Received February 15, 1999; in final form, October 4, 1999

**Abstract**—Alkali halide melt systems resulting from contact melting were studied by MD simulations. The simulation results were used to evaluate the diffusion coefficients, partial radial distribution functions, and velocity autocorrelation functions for various ionic compositions of the melt systems.

## INTRODUCTION

Over the past few decades, predicting the physico-chemical properties of melts has been a major challenge in materials science. Precise knowledge of equilibrium and nonequilibrium melt structure is critical for many technological applications. The discovery and investigation of contact melting offered a significant advance in this field [1, 2].

Contact melting is widely used in both scientific studies and technological applications to prepare and study melts graded in composition, determine interdiffusion coefficients and composition profiles, assess the effects of external influences on the structure and dynamics of melts, and investigate interfacial phenomena and phase transitions [3, 4].

Many of the issues concerning the scientific and technological aspects of contact melting can be clarified only by molecular (atomic) scale studies. In this paper, we review molecular dynamics (MD) approaches to studying contact melting and analyze earlier reported and new results.

We examined the ionic melts resulting from contact melting in alkali halide systems. These were chosen so as to highlight the effect of ionic composition on the kinetic and structural behavior of the melts:

(1) systems with a common anion, such as KBr–NaBr, NaI–KI, NaBr–RbBr, KBr–RbBr, and NaF–KF;

(2) systems with a common cation, such as NaI–NaBr, NaI–NaF, NaI–NaCl, KI–KBr, and KI–KF;

(3) mixed systems comprising sodium iodide and potassium halide, such as NaI–KF, NaI–KCl, NaI–KBr, and NaI–KCl.

## METHOD

In our studies, we used an upgraded MD simulation package [5] to analyze the trajectories of individual particles. The system included 256 particles enclosed in a cubic simulation box of length  $l$ . The equations of

Newtonian mechanics were integrated to obtain the coordinates and velocity of each ion. Periodic boundary conditions were employed; at each time step, the system was relaxed to thermal equilibrium. The initial velocities of the particles were set by a random number generator. The differential equations were solved in central differences. Interatomic interactions were considered additive and were described by a pair potential  $U(r)$  and force  $f(r)$  related by

$$f(r) = dU(r)/dr.$$

Simulations were carried out with Born–Huggins–Mayer (BHM) and Pauling pair potentials, which were used earlier to study KCl, KI, and KF [6]. Those results were utilized to test our software. The BHM potential has the form [6]

$$U(r_{ij}) = \frac{q_i q_j}{4\pi\epsilon_0 r_{ij}} + B_{ij} \exp(-\alpha_{ij} r_{ij}) - \frac{C_{ij}}{r_{ij}^6} - \frac{D_{ij}}{r_{ij}^8},$$
$$i, j = +, -,$$

where  $B_{ij} = \beta_{ij} b \exp[\alpha_{ij}(s_i + s_j)]$ ,  $b = 3.38 \times 10^{-20}$  J for any crystal and type of interaction,  $s_i$  and  $s_j$  are the radii of ionic species  $i$  and  $j$ , and  $\beta_{ij}$  is the so-called Pauling factor given by

$$\beta_{ij} = 1 + \frac{z_i}{n_i} + \frac{z_j}{n_j},$$

where  $n_i$  and  $n_j$  are the numbers of electrons in the outer shell (usually 8),  $z_i, z_j = \pm 1$ ,  $\alpha_{ij}$  is a constant (tabulated), and  $C_{ij}$  and  $D_{ij}$  are the van der Waals coefficients.

According to Pauling, the force acting between a pair of interacting ions  $i$  and  $j$  separated by distance  $r_{ij}$  is given by [7]

$$f(r_{ij}) = \frac{q_i q_j}{4\pi\epsilon_0 r_{ij}^2} \left[ 1 + \operatorname{sgn}(q_i q_j) \left( \frac{s_i + s_j}{r_{ij}} \right)^p \right], \quad i, j = \pm.$$

MD simulations were used to compute rms displacements, velocity autocorrelation functions, partial radial distribution functions (PRDFs), and diffusion coefficients.

The rms displacements of anions and cations were evaluated using the relation

$$Q_k(\tau) = \frac{1}{N_k} \sum_{i \in P_k} (R_i(\tau_0 + \tau) - R_i(\tau_0))^2, \quad \tau_1 < \tau < \tau_2,$$

$N_k$  is the number of ions of species  $k$ ,  $R_i$  is the position vector of ion  $i$ ,  $P_k$  is the set of numbers of species  $k$ ,  $\tau_0$  is the point in time at which two ionic systems are brought in contact, and  $\tau_1$  and  $\tau_2$  bound the time interval within which the  $Q_k(\tau)$  dependence can be considered linear.

The velocity autocorrelation function, characterizing the effect of interatomic interactions on the velocity of particles, is given by

$$Z(\tau) = \frac{1}{N} \left\langle \sum_{i=1}^N v_i(0)v_i(\tau) \right\rangle.$$

The diffusion coefficients were determined using the relation

$$D_k = \frac{6\tau}{Q_k(\tau) + C_k},$$

where  $\tau$  is the point in time after which the  $Q_k(\tau)$  dependence can be considered linear, and  $C_k$  is the linear extrapolation constant.

PRDFs were calculated by the relation

$$g_{ij}(r) = \frac{Vn_j(r)}{N_j 4\pi r_{ij}^2},$$

where  $r_{ij}$  is the distance between particles  $i$  and  $j$ ,  $V$  is the volume of the simulation box,  $N_j$  is the number of particles of species  $j$ , and  $n_j(r)$  is the number of particles of species  $j$  located distance  $r$  from a given particle of species  $i$ .

## RESULTS AND DISCUSSION

MD simulations were carried out for temperatures between 400 and 1200 K at 50-K intervals. The simulation box of side length  $l$  contained 64  $\text{Na}^+$ , 64  $\text{K}^+$ , and 128  $\text{I}^-$  ions. To test the simulation technique, we also considered pure NaI or KI.

By comparing simulation results with experimental data, the uncertainties in the positions of the first and second PRDF peaks were estimated to be 8 and 15%, respectively. The uncertainty in diffusion coefficients was 15%, and that in the velocity autocorrelation function was 9%.

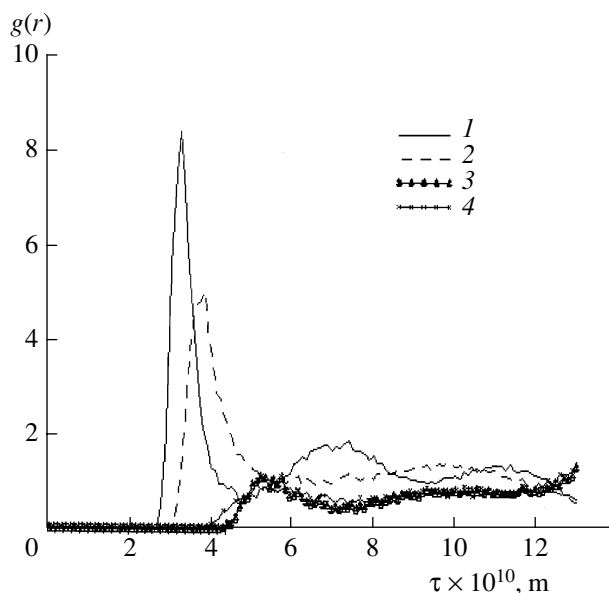


**Fig. 1.** (1)  $\text{Na}^+ - \text{I}^-$ , (2)  $\text{K}^+ - \text{I}^-$ , (3)  $\text{I}^- - \text{I}^-$ , and (4)  $\text{K}^+ - \text{Na}^+$  PRDFs at 860 K.

The properties of the melt were determined above the contact-melting temperature, which was evaluated from the jump in the diffusion coefficient.

**Systems with a common anion.** The PRDFs of the NaI–KI system at 860 K (Fig. 1) are typical of ionic melts. The nearest-neighbor-distance distributions are very sharp. The peaks arising from oppositely charged ions are located at smaller  $r$ : The next-nearest-neighbor-distance distributions are notably broadened, indicating much weaker second-neighbor interactions. The width of the second and third PRDF peaks increases with temperature.

The PRDF results for the other systems with a common anion are presented in Table 1. One can see that the height of the first PRDF peak increases with decreasing anion radius.

The oscillations in the velocity autocorrelation functions of the NaI–KI system are more pronounced for positive ions (Fig. 2). The oscillation period, of order  $10^{-13}$  s, is much shorter than the time during which the nearest neighbor environment remains unchanged. The curve for  $\text{I}^-$  crosses zero at  $\tau_0 = 2 \times 10^{-13}$  s. This time is notably longer than that for  $\text{Br}^-$  and

**Table 1.** First PRDF peak heights in systems with a common anion

System		NaF–KF	NaCl–KCl	NaBr–KBr	NaI–KI
Peak height	$\text{Na}^+ - \text{A}^-$	8.1	8.0	6.3	5.8
	$\text{K}^+ - \text{A}^-$	5.4	5.2	4.8	4.0

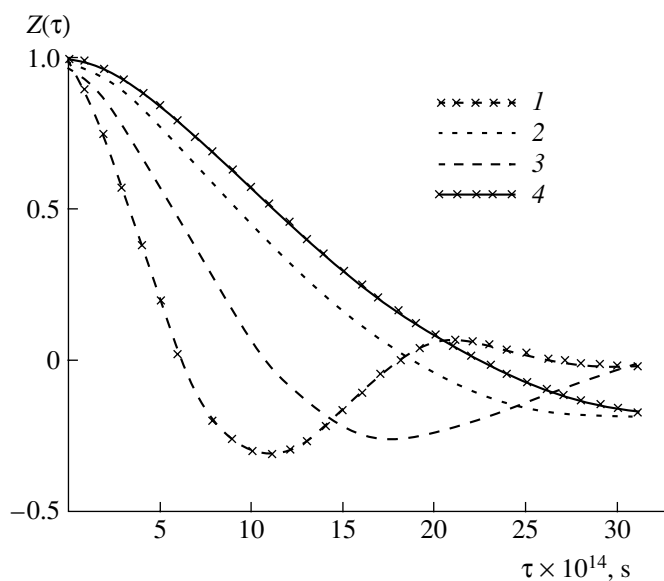


**Fig. 2.** Velocity autocorrelation functions in the NaI–KI system: (1) Na, (2) I (NaI), (3) K, (4) I (KI) ( $T = 860$  K).

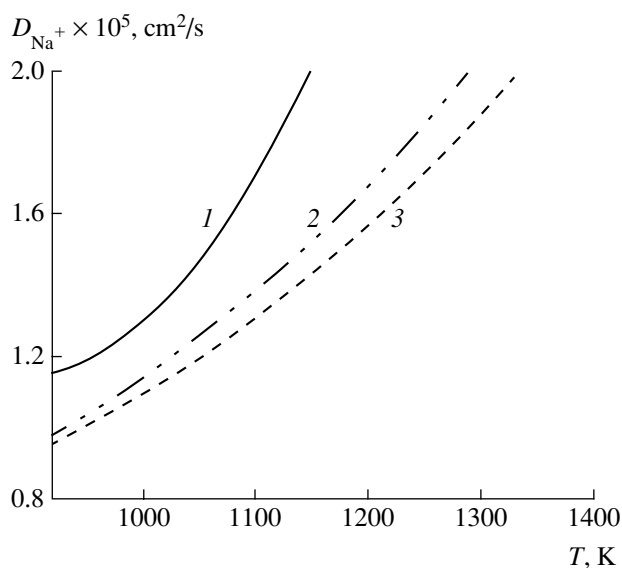


**Fig. 3.** Partial diffusion coefficient of  $\text{Na}^+$  vs. temperature for the systems (1) NaI–NaBr, (2) NaI–NaCl, (3) NaI–NaF.

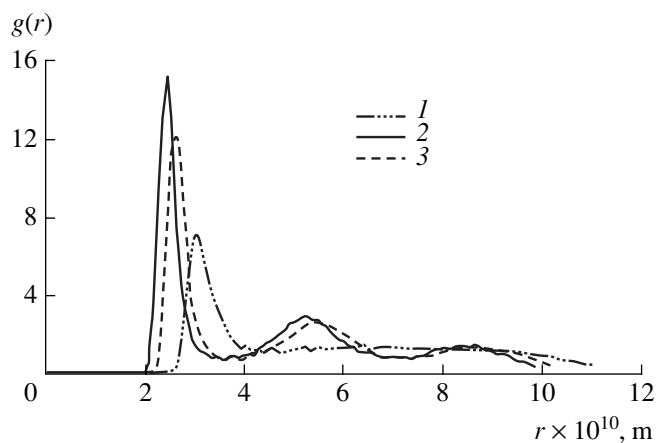


**Fig. 4.** (1)  $\text{Na}^+$ – $\text{Br}^-$ , (2)  $\text{Na}^+$ – $\text{F}^-$ , and (3)  $\text{Na}^+$ – $\text{Cl}^-$  PRDFs in the NaI–NaBr, NaI–NaF, and NaI–NaCl systems, respectively.

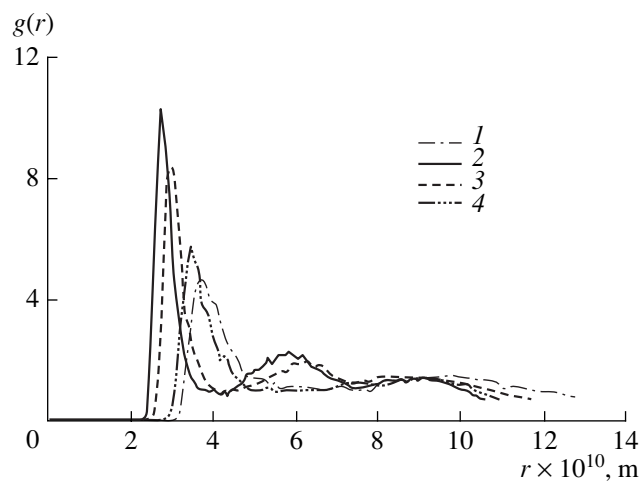


**Fig. 5.** (1)  $\text{K}^+$ – $\text{I}^-$ , (2)  $\text{K}^+$ – $\text{F}^-$ , (3)  $\text{K}^+$ – $\text{Cl}^-$ , and (4)  $\text{K}^+$ – $\text{Br}^-$  PRDFs in the NaI–KI, NaI–KF, NaI–KCl, and NaI–KBr systems, respectively.

$\text{Cl}^-$ , because the weight and radius of the  $\text{I}^-$  ion are notably larger. With increasing temperature, the oscillations become flatter,  $\tau_0$  rises, and the depth of the first minimum decreases.

Table 2 gives the diffusion coefficients in the systems with a common anion: NaF–KF, NaCl–KCl, NaBr–KBr, and NaI–KI. In all these systems, the diffusion coefficient rises exponentially with temperature. As the size of the anion rises, the diffusion coefficient of the cation increases, while that of the anion decreases.

**Systems with a common cation.** The diffusion coefficients, PRDFs, and velocity autocorrelation func-

tions in these systems were found to have a number of features in common.

Figure 3 shows the temperature dependences of the partial diffusion coefficient of  $\text{Na}^+$  in the systems NaI–NaBr, NaI–NaCl, and NaI–NaF. It can be seen that  $D_{\text{Na}^+}$  depends on the size of the second anion.

PRDF analysis provides further evidence that the major properties of the melt depend of the dimensions of the constituent ions. Figure 4 displays the  $\text{Na}^+$ – $\text{Br}^-$ ,  $\text{Na}^+$ – $\text{F}^-$ , and  $\text{Na}^+$ – $\text{Cl}^-$  PRDFs for the NaI–NaBr, NaI–NaF, and NaI–NaCl systems at a temperature 10 K higher than the contact-melting temperature, evaluated from the jump in the diffusion coefficient. These data

**Table 2.** Diffusion coefficients in systems with a common anion

Ion	$D \times 10^5, \text{cm}^2/\text{s}$			
	NaF–KF	NaCl–KCl	NaBr–KBr	NaI–KI
	1000 K		880 K	850 K
Na <sup>+</sup>	1.71	1.837	1.974	2.32
K <sup>+</sup>	1.2	1.38	1.856	3.27
A <sub>(Na)</sub> <sup>-</sup>	1.79	1.68	1.53	0.96
A <sub>(K)</sub> <sup>-</sup>	1.52	1.36	1.34	0.84

**Table 3.** Parameters of PRDFs in mixed and sodium halide systems

System	Ions	$g(r_{\text{max}})$	$r_{\text{max}} \times 10^{10}, \text{m}$	$r_{\text{max}} \times 10^{10}, \text{m}$
NaI–NaF	Na <sup>+</sup> –F <sup>-</sup>	15	2.4	1.9
NaI–NaCl	Na <sup>+</sup> –Cl <sup>-</sup>	12.2	2.5	2.1
NaI–NaBr	Na <sup>+</sup> –Br <sup>-</sup>	6.9	3.0	2.4
NaI–KF	K <sup>+</sup> –F <sup>-</sup>	10.3	2.8	2.3
NaI–KCl	K <sup>+</sup> –Cl <sup>-</sup>	8.5	3.1	2.5
NaI–KBr	K <sup>+</sup> –Br <sup>-</sup>	5.7	3.6	2.8
NaI–KI	K <sup>+</sup> –I <sup>-</sup>	4.3	3.8	3.1

demonstrate that the height of the first PRDF peak is inversely related to the weight and radius of the second anion: the peak for the Na<sup>+</sup>–F<sup>-</sup> pair is higher by a factor of 1.3 than that for the Na<sup>+</sup>–Cl<sup>-</sup> pair and by a factor of 2 than that for the Na<sup>+</sup>–Br<sup>-</sup> pair. Similar relationships were revealed for the second PRDF peaks. In addition, the peaks broaden somewhat as the weight and radius of the second anion increase.

**Mixed systems.** Simulations were carried out for the systems NaI–KBr, NaI–KF, NaI–KCl, and NaI–KI. Figure 5 shows the K<sup>+</sup>–F<sup>-</sup>, K<sup>+</sup>–I<sup>-</sup>, K<sup>+</sup>–Cl<sup>-</sup>, and K<sup>+</sup>–Br<sup>-</sup> PRDFs. The heights of the PRDF peaks are seen to be proportional to the size of the second anion.

The data presented in Table 3 indicate that the PRDF peaks in the systems containing a potassium halide are higher in comparison with the Na systems. Moreover, the latter are characterized by shorter interatomic distances ( $r_0$  and  $r_{\text{max}}$ ).

## CONCLUSION

Alkali halide melt systems were studied by MD simulations. The results show that, in the systems with a common anion, the diffusion coefficients of the cations increase and that of the anion decreases as the size of the anion rises. The height of the first PRDF peak increases with decreasing anion radius. The interionic distances in the melt increase with anion size.

In the systems with a common cation, the diffusion coefficient of the cation rises as the size of the second anion increases, while the heights of the PRDF peaks are inversely related to the size of the second anion.

## REFERENCES

1. Semenov, A.P., Pozdnyakov, V.V., and Kraposhina, L.B., *Trenie i kontaktnoe vzaimodeistvie grafita i almaza s metallami i splavami* (Friction and Contact Interaction of Graphite and Diamond with Metals and Alloys), Moscow: Nauka, 1974, p. 63.
2. Saratovkin, D.D. and Savintsev, P.A., Contact Melting as a Cause of the Low Melting Point of Eutectics, *Dokl. Akad. Nauk SSSR*, 1947, vol. 58, no. 9, pp. 1943–1944.
3. Popov, A.A., High-Speed Determination of Diffusivities in Molten Eutectic Systems, *Zavod. Lab.*, 1951, no. 6, pp. 684–688.
4. Savintsev, P.A., Zil'berman, P.F., and Savintsev, S.P., *Fizika kontaktnogo plavleniya* (Physics of Contact Melting), Nalchik: Kabardino-Balkarsk. Gos. Univ., 1987.
5. Znamenskii, V.S., Savintsev, P.A., and Zil'berman, P.F., Molecular Dynamics Study of Contact Melting, *Zh. Fiz. Khim.*, 1993, vol. 67, no. 7, pp. 1504–1507.
6. Sangster, M.J.L. and Dixon, M., Interionic Potentials in Alkali Halides and Their Use in Simulation of Molten Salts, *Adv. Phys.*, 1976, vol. 25, no. 3, pp. 247–342.
7. Hockney, R.W. and Eastwood, J.W., *Computer Simulation Using Particles*, New York: McGraw-Hill, 1984. Translated under the title *Chislennoe modelirovanie metodom chastits*, Moscow: Mir, 1987.